Single-Molecular-Level Study of Claudin-1-Mediated Adhesion

ARTICLE *in* LANGMUIR · FEBRUARY 2008

Impact Factor: 4.46 · DOI: 10.1021/la702436x · Source: PubMed

5 AUTHORS, INCLUDING:

Tong Seng Lim
Agency for Science, Technology and Researc…
19 PUBLICATIONS **149** CITATIONS
SEE PROFILE

Jaya Kausalya P
Agency for Science, Technology and Researc…
23 PUBLICATIONS **832** CITATIONS
SEE PROFILE

Walter Hunziker
Agency for Science, Technology and Researc…
130 PUBLICATIONS **6,870** CITATIONS
SEE PROFILE

C.T. Lim
National University of Singapore
388 PUBLICATIONS **13,002** CITATIONS
SEE PROFILE

Single-Molecular-Level Study of Claudin-1-Mediated Adhesion

Tong Seng Lim,[†,‡] Sri Ram Krishna Vedula,[§] P. Jaya Kausalya,[||] Walter Hunziker,[||] and Chwee Teck Lim*[,§]

*Bioinformatics Institute, A*STAR (Agency for Science, Technology and Research), 30 Biopolis Street, Singapore 138671, NUS Graduate School for Integrative Sciences and Engineering, 28 Medical Drive, Singapore 117456, Division of Bioengineering and Department of Mechanical Engineering, National University of Singapore, 9 Engineering Drive 1, Singapore 117576, and Institute of Molecular and Cell Biology, A*STAR (Agency for Science, Technology and Research), 61 Biopolis Drive, Singapore 138673*

Received August 7, 2007. In Final Form: September 28, 2007

Claudins are proteins that are selectively expressed at tight junctions (TJs) of epithelial cells where they play a central role in regulating paracellular permeability of solutes across epithelia. However, the role of claudins in intercellular adhesion and the mechanism by which they regulate the diffusion of solutes are poorly understood. Here, using single molecule force spectroscopy, the kinetic properties and adhesion strength of homophilic claudin-1 interactions were probed at the single-molecule level. Within the range of tested loading rates (10^3-10^5 pN/s), our results showed that homophilic claudin-1 interactions have a reactive compliance of 0.363 ± 0.061 nm and an unstressed dissociation rate of 1.351 ± 1.312 s^{-1}. This is more than 100-fold greater than that of E-cadherin. The weak and short-lived interactions between claudin-1 molecules make them highly unstable and dynamic in nature. Such a dynamic interaction is consistent with a model where breaking and resealing of TJ strands regulate the paracellular diffusion of solutes.

Introduction

Intercellular junctions play an extremely important role in maintaining homeostasis in multicellular organisms. The epithelial intercellular adhesion complex consists of several components that include the adherens junctions (AJs), tight junctions (TJs), gap junctions, and desmosomes. TJs constitute the most apical junctional complex in epithelial cells.[1] Apart from acting as barriers to paracellular diffusion of extracellular solutes,[2] they also restrict the apical proteins from diffusing to the basolateral membrane,[3,4] regulate cell proliferation and differentiation,[5] and have been recently identified as coreceptors for hepatitis C virus.[6]

In recent years, the adhesion behavior of E-cadherins (localizing at AJs) has been extensively investigated at the levels of both the cell and single molecule using flow chamber assay,[7] dual pipet assay,[8,9] cell aggregation assay,[10] atomic force microscopy (AFM),[11,12] and surface force analysis.[13] While the role of E-cadherins at AJs is well established and has been characterized in some detail, little is known about the strength of adhesion forces mediated by TJ proteins.

Claudins (Cldns) comprise a protein family of 24 members in mammals that have been identified as major tetraspan transmembrane proteins localized at TJs.[14−16] Structurally, Cldns contain two extracellular loops and four transmembrane regions. The two extracellular loops of Cldns belonging to adjacent cells interact to form the paracellular TJ strands. Using cell aggregation assays, claudin-1 (Cldn1), claudin-2, and claudin-3 were found to exhibit Ca^{2+}-independent adhesion activities.[17] However, the strength and kinetics of the interactions mediated by Cldns have not been characterized. In this study we have used single-molecule force spectroscopy to gain insight into the kinetics of Cldn-mediated interactions using full-length human Cldn1, tagged with GST (glutathione S-transferase) on the N-terminal end (GST−Cldn1), as a representative model.

Our results show that dissociation of the homophilic Cldn1/Cldn1 bond involves a single energy barrier in the range of loading rates between 10^3 and 10^5 pN/s. Comparison of interaction kinetics revealed that Cldn1 dissociates at a much faster rate than E-cadherins. This supports the fact that E-cadherin is more important in providing mechanical stability to epithelial cell junctions. The weak and short-lived interactions between claudin-1 molecules are highly unstable and dynamic in nature. The dynamic nature of these interactions is consistent with the model in which breaking and resealing of TJ strands regulate the paracellular diffusion of solutes across epithelia.[18,19]

* To whom correspondence should be addressed. Phone: +65 6516 7801. E-mail: ctlim@nus.edu.sg.

[†] Bioinformatics Institute.

[‡] NUS Graduate School for Integrative Sciences and Engineering.

[§] National University of Singapore.

[||] Institute of Molecular and Cell Biology.

(1) Tsukita, S.; Furuse, M.; Itoh, M. *Nat. Rev. Mol. Cell Biol.* **2001**, *2*, 285.

(2) Kovbasnjuk, O.; Leader, J. P.; Weinstein, A. M.; Spring, K. R. *Proc. Natl. Acad. Sci. U.S.A.* **1998**, *95*, 6526.

(3) Schneeberger, E. E.; Lynch, R. D. *Am. J. Physiol.* **1992**, *262*, L647.

(4) Gumbiner, B. M. *J. Cell Biol.* **1993**, *123*, 1631.

(5) Matter, K.; Balda, M. S. *Nat. Rev. Mol. Cell Biol.* **2003**, *4*, 225.

(6) Evans, M. J.; von Hahn, T.; Tscherne, D. M.; Syder, A. J.; Panis, M.; Wolk, B.; Hatziioannou, T.; McKeating, J. A.; Bieniasz, P. D.; Rice, C. M. *Nature* **2007**, *446*, 801.

(7) Perret, E.; Benoliel, A. M.; Nassoy, P.; Pierres, A.; Delmas, V.; Thiery, J. P.; Bongrand, P.; Feracci, H. *EMBO J.* **2002**, *21*, 2537.

(8) Chu, Y. S.; Eder, O.; Thomas, W. A.; Simcha, I.; Pincet, F.; Ben-Ze'ev, A.; Perez, E.; Thiery, J. P.; Dufour, S. *J. Biol. Chem.* **2006**, *281*, 2901.

(9) Chu, Y. S.; Thomas, W. A.; Eder, O.; Pincet, F.; Perez, E.; Thiery, J. P.; Dufour, S. *J. Cell Biol.* **2004**, *167*, 1183.

(10) Duguay, D.; Foty, R. A.; Steinberg, M. S. *Dev. Biol.* **2003**, *253*, 309.

(11) Panorchan, P.; Thompson, M. S.; Davis, K. J.; Tseng, Y.; Konstantopoulos, K.; Wirtz, D. *J. Cell Sci.* **2006**, *119*, 66.

(12) Perret, E.; Leung, A.; Feracci, H.; Evans, E. *Proc. Natl. Acad. Sci. U.S.A.* **2004**, *101*, 16472.

(13) Sivasankar, S.; Gumbiner, B.; Leckband, D. *Biophys. J.* **2001**, *80*, 1758.

(14) Furuse, M.; Fujita, K.; Hiiragi, T.; Fujimoto, K.; Tsukita, S. *J. Cell Biol.* **1998**, *141*, 1539.

(15) Morita, K.; Furuse, M.; Fujimoto, K.; Tsukita, S. *Proc. Natl. Acad. Sci. U.S.A.* **1999**, *96*, 511.

(16) Loh, Y. H.; Christoffels, A.; Brenner, S.; Hunziker, W.; Venkatesh, B. *Genome Res.* **2004**, *14*, 1248.

(17) Kubota, K.; Furuse, M.; Sasaki, H.; Sonoda, N.; Fujita, K.; Nagafuchi, A.; Tsukita, S. *Curr. Biol.* **1999**, *9*, 1035.

(18) Sasaki, H.; Matsui, C.; Furuse, K.; Mimori-Kiyosue, Y.; Furuse, M.; Tsukita, S. *Proc. Natl. Acad. Sci. U.S.A.* **2003**, *100*, 3971.

(19) Matsuda, M.; Kubo, A.; Furuse, M.; Tsukita, S. *J. Cell Sci.* **2004**, *117*, 1247.

10.1021/la702436x CCC: $40.75
Published on Web 12/21/2007

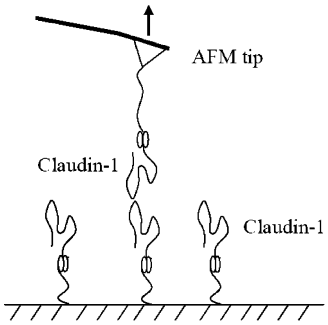

Figure 1. Schematic of the AFM experimental setup. Recombinant GST−Cldn1 was linked to the AFM tip using anti-GST antibody (see the Materials and Methods). GST−Cldn1 immobilized on a glass coverslip was probed using these functionalized tips. The arrow indicates the direction of pulling in the AFM experiment. GST = glutathione S-transferase.

Materials and Methods

Protein Immobilization and Cantilever Functionalization. Silicon nitride tips (model MLCT-AUNM, Veeco, Santa Barbara, CA) were first cleaned by irradiating them with UV. Following incubation in a mixture of 30% H_2O_2/70% H_2SO_4 for 30 min, the tips were washed in ddH_2O and dried. The tips were then silanized by immersing them in a 4% solution of APTES ((3-aminopropyl)-triethoxysilane in acetone; Sigma) for 3 min. Mouse anti-GST antibody (5 μg/mL, Invitrogen) was coupled to the silanized tips using BS^3 (bis(sulfosuccinimidyl) suberate; 2 mg/mL, Pierce) as a cross-linker. The reaction was quenched using 1 M Tris buffer. To confirm that anti-GST was efficiently linked to the silanized tips, Alexa 488 labeled goat anti-mouse antibody (Molecular Probes, Invitrogen) was used to stain the anti-GST-coupled tips. It was found that Alexa 488 labeled goat anti-mouse antibody bound efficiently to the anti-GST-coupled silanized tips but not to silanized tips treated with only BS^3 and quenched using 1 M Tris buffer. The tips were then incubated in a solution of recombinant full-length GST−Cldn1 (50 μg/mL, Abnova, Taiwan) for 2 h. Unbound GST−Cldn1 was washed off with PBS. The tips were blocked in 1% BSA before the experiments.[20] GST−Cldn1 was immobilized on glass coverslips using the same procedure as described above. For control experiments, all steps were similar except that incubation in GST−Cldn1 was omitted. For blocking experiments, the tips and coverslips were incubated with antibody to the cytoplasmic domain of Cldn1 (1.25 μg/mL, Invitrogen) for 30 min. They were then washed to remove any unbound antibody.

Dynamic Force Spectroscopy Experiments. Force curves were acquired on a MultiMode PicoForce AFM instrument (Veeco) coupled to an upright microscope at room temperature using a fluid cell. Cantilevers with a nominal spring constant of 0.01−0.03 N/m were used for obtaining force plots. Prior to obtaining force curves, the spring constant was determined using the thermal tune module. GST−Cldn1 immobilized on the glass coverslips were probed with GST−Cldn1-functionalized cantilevers. Force plots were obtained at different reproach velocities (1, 2.5, 5, and 10 μm/s). To minimize the number of adhesion events and maximize the probability of obtaining single-bond adhesion events, a contact force of 200 pN and a contact time of 1 ms were used. The target adhesion frequency was 30%, which would give a >85% probability of the rupture forces being due to single bond rupture.[20] Force curves showing only single bond failure were analyzed for the magnitude of the rupture events and the apparent loading rate (defined as the slope of the retrace curve prior to the rupture event multiplied by the reproach velocity) using MATLAB version 6.5 (The MathWorks, Natick, MA). Following Hanley et al.[21] and Panorchan et al.,[11] rupture force measurements were partitioned by using binning windows of 100 pN/s for loading rates between 100 and 1000 pN/s and binning windows of 1000 pN/s for loading rates between 1000 and 10000 pN/s. Each bin yields a peak force by Gaussian fitting. By plotting the peak force as a function of the loading rate, the unstressed dissociation rate and reactive compliance for the molecular interactions were extracted (see the Results). These parameters characterize the binding interactions between homophilic Cldn1 proteins at the single-molecule level.

(20) Hanley, W.; McCarty, O.; Jadhav, S.; Tseng, Y.; Wirtz, D.; Konstantopoulos, K. *J. Biol. Chem.* **2003**, *278*, 10556.
(21) Hanley, W. D.; Wirtz, D.; Konstantopoulos, K. *J. Cell Sci.* **2004**, *117*, 2503.

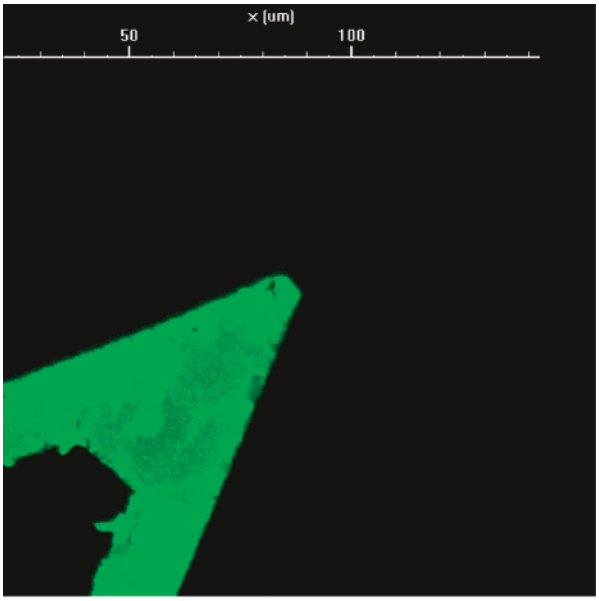

(a)

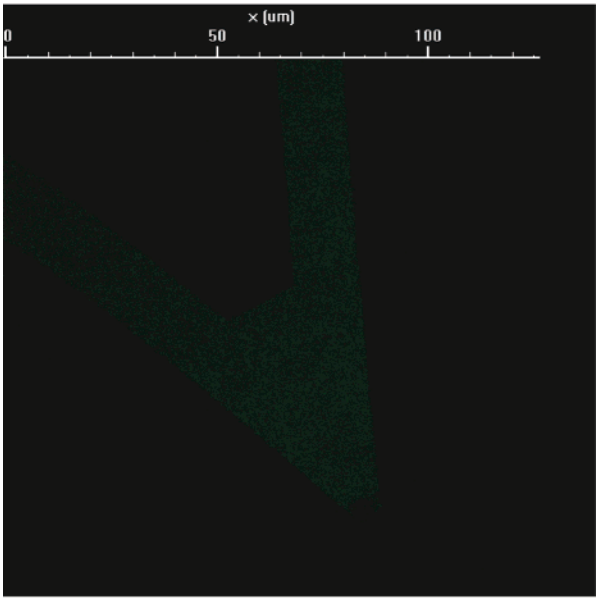

(b)

Figure 2. Confocal images of silanized AFM cantilevers functionalized (a) with anti-GST and (b) without anti-GST incubated with Alexa 488 labeled antibody (see the Materials and Methods for details). Both images were acquired under similar conditions (pixel dwell time, laser power, and gain).

Results

Measurement of Cldn1/Cldn1 Interaction Forces and Extraction of the Kinetic Parameters of Interaction Using the Bell−Evans Model. Binding interactions between apposing Cldn1 molecules were characterized at the level of a single

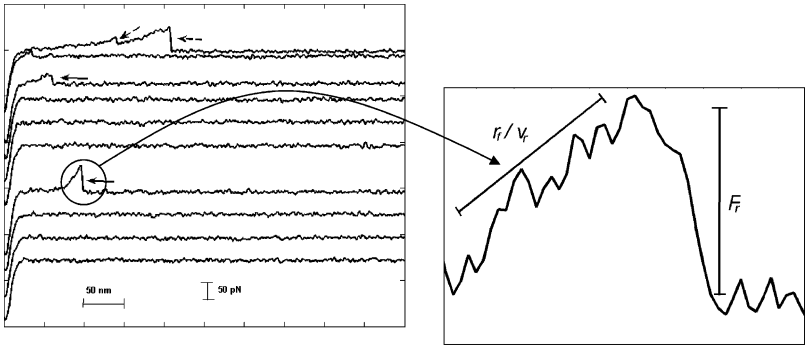

Figure 3. Force curves showing rupture of individual bonds mediated by Cldn1/Cldn1 interactions. (a) Typical force−distance curves obtained between a tip functionalized with GST−Cldn1 and GST−Cldn1 immobilized on glass coverslips. Arrows indicate rupture of homophilic Cldn1/Cldn1 interactions. The curves show no rupture event, a single bond rupture event, or occasionally multiple bond rupture events (dashed arrows). Only curves showing a single clear rupture event were used for generating the histograms. (b) Enlarged force−distance curves prior to bond rupture. The slope of the curve just before rupture multiplied by the reproach velocity (V_r, μm/s) defines the loading rate (r_f, pN/s). The height of the rupture event defines the magnitude of the rupture force (F_r, pN).

Table 1. Sample and Control Experiments To Study Molecular Interactions of Homophilic Cldn1/Cldn1 Interactions

interaction type	AFM tip[a]	antibody to Cldn1	glass substrate[a]
1. AntiGST_AntiGST	anti-GST	−	anti-GST
2. AntiGST_Cldn1	anti-GST	−	GST−Cldn1
3. Cldn1_Cldn1_Ab	GST−Cldn1	+	GST−Cldn1
4. Cldn1_Cldn1	GST−Cldn1	−	GST−Cldn1

[a] Key: anti-GST, antibody targeting GST; GST−Cldn1, recombinant GST-tagged Cldn1 protein (see the Materials and Methods for details about the immobilization of proteins onto the AFM tip and glass substrate).

Table 2. Comparison of Adhesion Kinetics of Homophilic Mediated by E-Cadherin and Cldn1

molecular pair	bond strength,[a] f^* (pN)	rate of dissociation,[a] k_{off}^0 (s^{-1})	reactive compliance,[a] x_β (nm)
E-cadherin/E-cadherin[b]	39, 51	0.01	0.8
	55, 62	10^{-6}−10^{-5}	1.3−1.1
Cldn1/Cldn1	21, 48	1.35 ± 1.31	0.36 ± 0.06

[a] The first and second values of the bond strength (f^*) correspond to loading rates of 10^2 and 10^3 pN/s, respectively. The reactive compliance, x_β, and the unstressed bond dissociation rate, k_{off}^0, were fitted from the loading rate curve (Figure 5) using eq 1 and using the nonlinear least-squares method with the trust-region algorithm.[42] The extracted kinetic parameters are listed as the mean ± standard deviation. [b] The E-cadherin data are obtained from a previous study,[12] where E-cadherin was shown to exhibit a hierarchy of mechanical strengths corresponding to two bound states.

molecule using AFM (Figure 1).[11,21,22] The interaction was established by bringing the GST−Cldn1-functionalized cantilever in close contact to a glass coverslip coated with GST−Cldn1 (see the Materials and Methods). The functionalization of the tips was confirmed using Alexa 488 labeled goat anti-mouse antibody (Molecular Probes, Invitrogen). Confocal images showed that anti-GST antibody was efficiently coupled to the AFM tips (Figure 2). In single-molecule force spectroscopy experiments, the contact force and contact time are crucial for measuring discrete deadhesion forces with molecular resolution.[22] When a contact force of 200 pN and contact time of 1 ms were used, <30% of the force−distance curves showed bond rupture events. On the basis of Poisson statistics,[23] the low frequency of these deadhesion events ensured a >85% probability of the rupture being due to a single bond.

Upon retraction of the cantilever, force as a function of pulling distance was recorded.[24] Typical force−distance curves are shown in Figure 3a. For each reproach velocity, hundreds of force−distance curves (n > 500) were collected and analyzed to extract the rupture force and loading rate (F_r, r_f, Figure 3b). These were subsequently pooled into histograms (Figure 4). Binding was specific because the adhesion frequency was significantly reduced in control experiments performed using AFM tips functionalized with only anti-GST protein. Furthermore, a blocking experiment using antibody specifically targeting the C-terminus of Cldn1 significantly reduced the binding frequency (Table 1, Figure 4). Though it was surprising that an antibody to the C-terminal of Cldn1 blocked these interactions, it is very likely that the antibody provided steric hindrance, preventing the Cldn1 loops from coming in contact with one another.

Biophysical parameters characterizing the interaction kinetics of homophilic Cldn1/Cldn1 interactions were calculated using the Bell−Evans model.[25,26] This model relates the bond rupture force to the loading rate applied to the bond. It has previously been used to characterize binding interactions of VE-cadherin/VE-cadherin,[27] N-cadherin/N-cadherin, and E-cadherin/E-cadherin.[11,12] In the model, the "bond strength" (defined as the most probable rupture force, f^*) shows a linear relation to the natural logarithm of the loading rate (r_f, eq 1):

$$f^* = \frac{k_B T}{x_\beta} \ln\left(\frac{x_\beta}{k_{off}^0 k_B T}\right) + \frac{k_B T}{x_\beta} \ln(r_f) \qquad (1)$$

where k_B is the Boltzmann constant and T is the absolute temperature. Using the fitted loading rate curve of rupture force vs loading rate (Figure 5) and Bell−Evans model (eq 1), we could extract the unstressed dissociation constant (k_{off}^0) and the reactive compliance (x_β). Although AFM measurements were performed under a nonzero loading rate, the unstressed dissociation constant could be computed by extrapolating the data to zero rupture force.

As expected, within the range of tested loading rates (10^3−10^5 pN/s), the strength of the Cldn1/Cldn1 bond increased linearly

(22) Benoit, M.; Gabriel, D.; Gerisch, G.; Gaub, H. E. *Nat. Cell Biol.* **2000**, *2*, 313.
(23) Chesla, S. E.; Selvaraj, P.; Zhu, C. *Biophys. J.* **1998**, *75*, 1553.
(24) Vedula, S. R.; Lim, T. S.; Kausalya, P. J.; Hunziker, W.; Rajagopal, G.; Lim, C. T. *Mol. Cell Biomech.* **2005**, *2*, 105.
(25) Bell, G. I. *Science* **1978**, *200*, 618.
(26) Evans, E.; Ritchie, K. *Biophys. J.* **1997**, *72*, 1541.
(27) Baumgartner, W.; Hinterdorfer, P.; Ness, W.; Raab, A.; Vestweber, D.; Schindler, H.; Drenckhahn, D. *Proc. Natl. Acad. Sci. U.S.A.* **2000**, *97*, 4005.

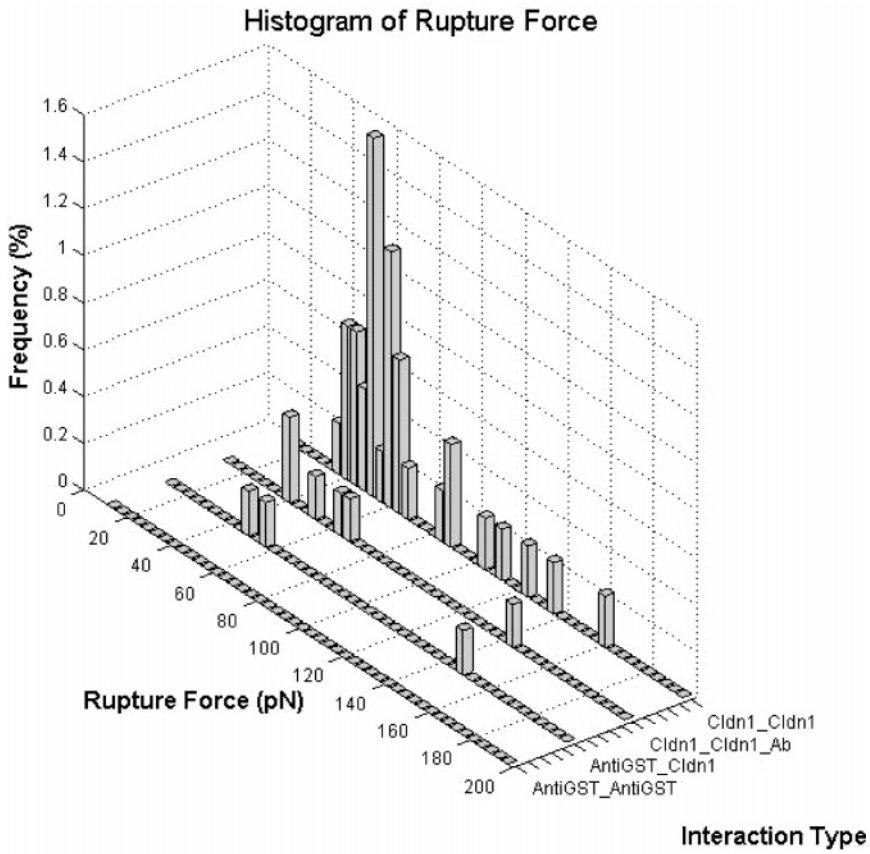

Figure 4. Rupture force histograms obtained between a tip functionalized with only anti-GST antibody and anti-GST antibody immobilized on a glass coverslip (AntiGST_AntiGST), between a tip functionalized with only anti-GST antibody and Cldn1 immobilized on a glass coverslip (AntiGST_Cldn1), and between a tip functionalized with GST−Cldn1 and GST−Cldn1 immobilized on a glass coverslip in the presence (Cldn1_Cldn1_Ab) or absence (Cldn1_Cldn1) of antibody to Cldn1 at a reproach velocity of 5 μm/s. GST = glutathione S-transferase. The interacting species for the different experiments are listed in Table 1.

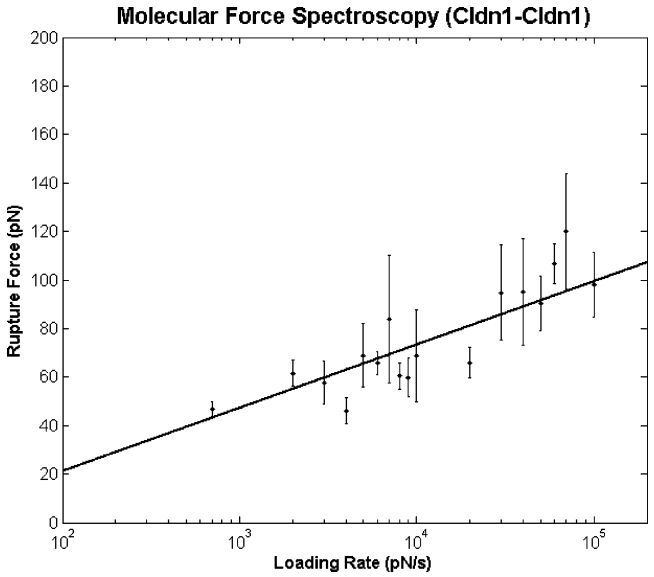

Figure 5. Molecular force spectroscopy of homophilic Cldn1/Cldn1 interactions. The most probable rupture force (mean ± standard error) was plotted as a function of the loading rate. By extrapolating it to zero rupture force, the unstressed dissociation rate ($k_{off}^0 = 1.351 \pm 1.312$ s^{-1}) and reactive compliance ($x_\beta = 0.363 \pm 0.061$ nm) for the Cldn1/Cldn1 interaction were extracted (see Table 2).

with the natural logarithm of the loading rate (Figure 5). The strength of the Cldn1/Cldn1 bond was 21 pN for a loading rate of 10^2 pN/s and 48 pN for a loading rate of 10^3 pN/s (Figure 5, Table 2). The unstressed dissociation rate and reactive compliance of the Cldn1/Cldn1 bond were found to be 1.351 ± 1.312 s^{-1} and 0.363 ± 0.061 nm, respectively. The kinetic parameters for Cldn1-mediated homophilic interactions are listed in Table 2 along with those of E-cadherin-mediated interactions for comparison. Cldn1 exists in only a single stable bound state, in contrast to E-cadherin-mediated adhesion, which was shown to exhibit a hierarchy of mechanical strengths with two bound states.[12] The lower strength and higher dissociation rate of the Cldn1/Cldn1 bond implies that it is less stable than the E-cadherin/E-cadherin bond.

Monte Carlo Simulation. Monte Carlo (MC) simulations of receptor−ligand bond rupture under constant loading rates were performed to further corroborate our experimental results with Bell's model predictions using a previously described procedure.[11,20] A total of 1000 rupture forces ($F_{rup} = (r_f)(n\Delta t)$) were calculated for which the probability of bond rupture, P_{rup}

$$P_{rup} = 1 - \exp\left[-\frac{k_{off}^0 k_B T}{x_b r_f}\left(\exp\left(\frac{x_b r_f n\Delta t}{k_B T}\right) - 1\right)\right] \qquad (2)$$

was greater than P_{ran}, a random number between 0 and 1. Here $n\Delta t$ is the time interval needed to break a bond and Δt is the time step ($\Delta t = 1$ ms was used in the simulation). The values of the unstressed dissociation rate ($k_{off}^0 = 1.351 \pm 1.312$ s^{-1}) and reactive compliance ($x_\beta = 0.363 \pm 0.061$ nm) obtained experimentally above were used in the simulation. Results obtained from the simulation agreed well with the experimental results (Figure 6b). The loading rate (logarithm scale) was assumed to be normally distributed within the simulation range

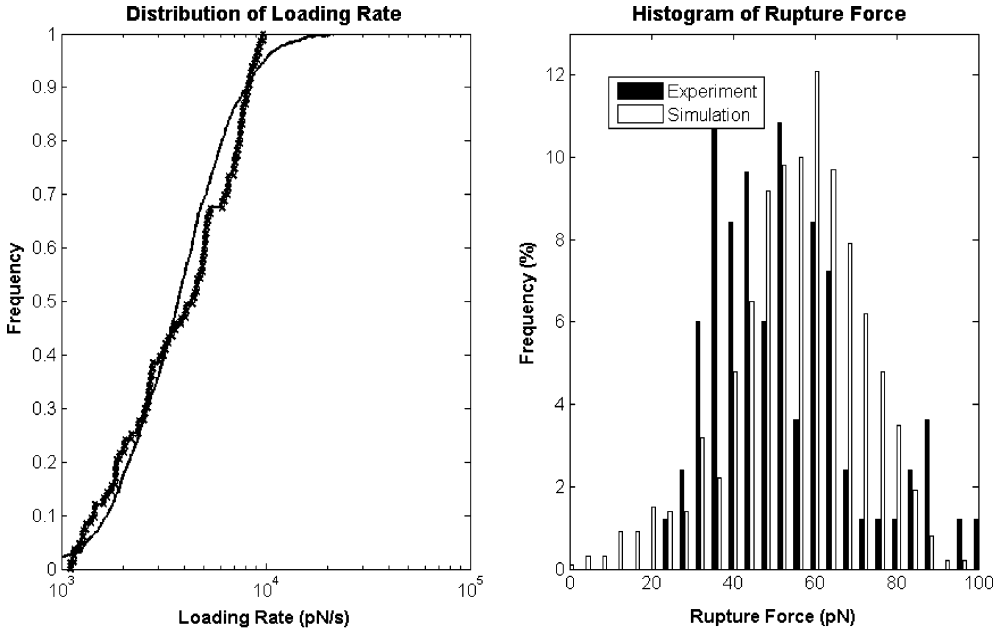

Figure 6. Comparison of the experimental and theoretical rupture force distribution of the Cldn1/Cldn1 interaction: (a) empirical cumulative distribution function of the loading rate for experimental data (line with times signs) and MC simulations (continuous line), (b) experimental (black) and theoretical (white) histograms of rupture forces to break a single Cldn1/Cldn1 bond at loading rates between 10^3 and 10^4 pN/s. MC simulations, which were conducted using the Bell model unstressed off rate ($k_{off}^0 = 1.351 \pm 1.312$ s^{-1}) and reactive compliance ($x_\beta = 0.363 \pm 0.061$ nm) obtained from force spectroscopy experiments, were consistent with the experimental data and further indicate that only one single type of bond was analyzed.

of loading (χ^2 test, $p < 0.05$). This assumption is valid and will not cause significant bias to the simulation as the cumulative distribution function of the loading rate fits well between the experimental data and MC simulation (Figure 6a). Since the simulated distribution was obtained using a single dissociation rate and reactive compliance, the good agreement between the computational and experimental distributions indicates that the rupture event is mainly caused by breaking of a single bond and not from the breaking of multiple bonds.

Discussion

Claudins belong to a family of tetraspan cell−surface adhesion molecules that are selectively expressed at TJs. Although TJs play an important role in regulating paracellular transport of solutes,[28] little is known about the strength and kinetics of the interactions mediated by them. Here, using GST−Cldn1 as a representative model of Cldns, we have probed homophilic Cldn interactions at the level of a single molecule. The analysis presented here examined the contribution of individual molecules instead of describing global cellular adhesion behavior which has been measured previously using flow chambers,[29] dual pipet assay,[8,9] or cell aggregation assays.[10]

To place our single-molecule measurement of Cldn interactions in context, we compared the extracted kinetic parameters with those mediated by E-cadherins (Table 2). E-cadherins play a key role in stabilizing intercellular adhesions and influencing cellular processes such as migration, differentiation, and carcinogenesis.[30] Cldn1/Cldn1 bonds were found to be relatively weak (∼21 and 48 pN) in comparison to E-cadherin bonds (∼39 and 51 pN and ∼55 and 62 pN for different binding configurations) at loading rates of 10^2 and 10^3 pN/s, respectively. This suggests that AJs are the more important components for stabilizing intercellular adhesion.

The E-cadherin/E-cadherin complex was previously found to exhibit a hierarchy of mechanical strengths with two bound states.[12] Here, we showed that there is only a single stable bound state for the dissociation of the Cldn1/Cldn1 complex within the range of tested loading rates (10^3−10^5 pN/s) (Figure 7). Using the unstressed dissociation rate (k_{off}^0) and reactive compliance (x_β) as listed in Table 2, the geometry of the conceptual energy landscape for the dissociation pathway can be constructed on the basis of these kinetic parameters.[25,31,32] The energy height (ΔE) for the activation barrier is written as

$$\Delta E = -k_B T(\ln k_{off}^0 - A) \quad (3)$$

where k_{off}^0 is the unstressed dissociation rate and A is a constant derived from frequency prefactors in the dissociation process. Although the absolute energy levels of each barrier from the level of the bound state cannot be confirmed due to the uncertainty of the constant A, however, the absolute positions of the energy barriers can be determined from x_β. To compare the topography of the energy landscape of the dissociation of Cldn1/Cldn1 and E-cadherin/E-cadherin, the geometric locations of their bound states were plotted on the same reactive coordinates (Figure 7). However, it should be stressed that dissociation pathways for Cldn1/Cldn1 and E-cadherin/E-cadherin interactions may take different reactive coordinates in general.

It has been proposed that Cldns form aqueous pores within tight junction strands which regulate paracellular diffusion of

(28) Van Itallie, C. M.; Anderson, J. M. *Annu. Rev. Physiol.* **2006**, *68*, 403.
(29) Niessen, C. M.; Gumbiner, B. M. *J. Cell Biol.* **2002**, *156*, 389.
(30) Adams, C. L.; Nelson, W. J. *Curr. Opin. Cell Biol.* **1998**, *10*, 572.
(31) Merkel, R.; Nassoy, P.; Leung, A.; Ritchie, K.; Evans, E. *Nature* **1999**, *397*, 50.
(32) Evans, E. *Annu. Rev. Biophys. Biomol. Struct.* **2001**, *30*, 105.
(33) Tsukita, S.; Furuse, M. *J. Cell Biol.* **2000**, *149*, 13.
(34) Van Itallie, C. M.; Anderson, J. M. *Physiology (Bethesda)* **2004**, *19*, 331.

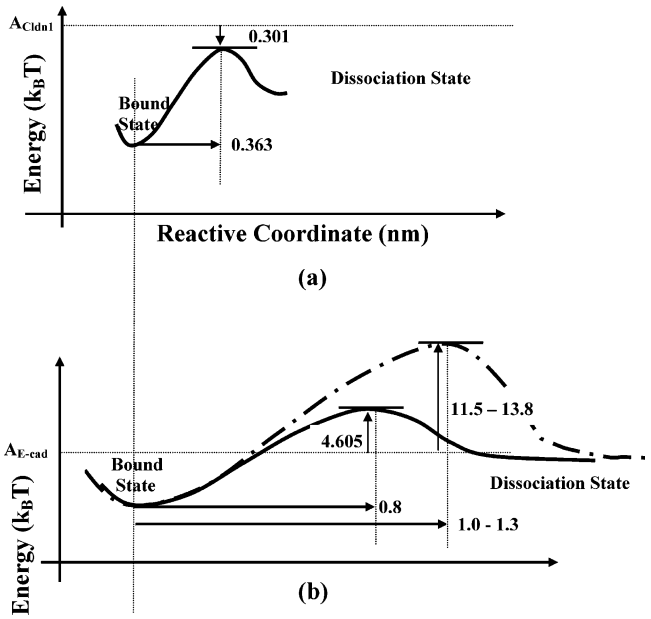

Figure 7. Comparison of conceptual energy landscapes of the dissociation pathway between homophilic Cldn1/Cldn1 and E-cadherin/E-cadherin interactions: (a) single energy activation barrier for the Cldn1/Cldn1 dissociation pathway using the kinetic parameters obtained from dynamic force spectroscopy within the range of tested loading rates (10^3-10^5 pN/s) (Table 2), (b) energy activation barriers for the E-cadherin/E-cadherin dissociation pathway, which was constructed on the basis of a previous dynamic force spectroscopy study.[12] A_{Cldn1} and A_{E-cad} are constants derived from frequency factors in the dissociation processes of Cldn1/Cldn1 and E-cadherin/E-cadherin bonds, respectively. In general, dissociation pathways for Cldn1/Cldn1 and E-cadherin/E-cadherin interactions may take different reactive coordinates. Here, the geometric locations for their bound states were plotted on the same reactive coordinates for the purpose of comparison. All dissociation pathways were not sketched to scale. k_B = Boltzmann constant, and T = absolute temperature.

solutes.[28,33,34] Also, L-fibroblasts transfected with Cldns have been shown to form strands that dynamically associate with one another in an end-to-side and side-to-side manner.[18] The fast dissociation rate of Cldn1 (100-fold greater than that of E-cadherin) strongly supports the fact that Cldn1-mediated interactions are weak and highly unstable. This could significantly contribute to the ability of Cldns to determine the paracellular permeability of epithelial monolayers to solutes.

In force spectroscopy experiments involving recombinant and isolated proteins, one of the primary concerns is whether the natural structure of the protein being investigated is preserved. It has been shown previously that isolated and purified Cldn1 tagged with GST and an Fc fragment retain their structure and are suitable for in vitro experiments.[35] Understanding interactions mediated by Cldns is important not only because of the role that they play in regulating paracellular transport of solutes and intercellular adhesion but also because of their role in acting as coreceptors for the entry of hepatitis C virus.[6] Given that both homophilic and heterophilic interactions can form between different Cldn species,[34,36,37] it will be interesting to see the differences in the kinetics of interactions occurring between different Cldn species in TJs. In the future, single-molecule analysis could be performed on other structural components of TJs,[38] such as occludin[39] and junctional adhesion molecules (JAMs),[40,41] to gain a better perspective of how the interaction kinetics of different adhesion molecules affect the organization and functioning of TJs.

Acknowledgment. This work is supported by the Biomedical Research Council (BMRC), Agency for Science, Technology & Research (A*STAR), Singapore.

LA702436X

(35) Tanaka, M.; Kamata, R.; Sakai, R. *EMBO J.* **2005**, *24*, 3700.
(36) Turksen, K.; Troy, T. C. *J. Cell Sci.* **2004**, *117*, 2435.
(37) Furuse, M.; Sasaki, H.; Tsukita, S. *J. Cell Biol.* **1999**, *147*, 891.
(38) Gonzalez-Mariscal, L.; Betanzos, A.; Nava, P.; Jaramillo, B. E. *Prog. Biophys. Mol. Biol.* **2003**, *81*, 1.
(39) Furuse, M.; Hirase, T.; Itoh, M.; Nagafuchi, A.; Yonemura, S.; Tsukita, S. *J. Cell Biol.* **1993**, *123*, 1777.
(40) Martin-Padura, I.; Lostaglio, S.; Schneemann, M.; Williams, L.; Romano, M.; Fruscella, P.; Panzeri, C.; Stoppacciaro, A.; Ruco, L.; Villa, A.; Simmons, D.; Dejana, E. *J. Cell Biol.* **1998**, *142*, 117.
(41) Williams, L. A.; Martin-Padura, I.; Dejana, E.; Hogg, N.; Simmons, D. L. *Mol. Immunol.* **1999**, *36*, 1175.
(42) Gilles, L.; Vogel, C. R.; Ellerbroek, B. L. *J. Opt. Soc. Am. A* **2002**, *19*, 1817.